Synchrotron-betatron coupling due to monochromatization

Stefania Petracca
University of Sannio, Benevento, Italy
and INFN, Salerno, Italy

Kohji Hirata*
Sokendai, The Graduate University for Advanced Studies, Hayama, Japan
(Received 2 August 2000; published 18 June 2001)

The effects of large dispersion at the interaction point are discussed within the linear approximation of the beam-beam force. The synchrotron and betatron motions affect each other. Synchrotron and betatron tune shifts as well as bunch-length and energy-spread modifications appear, among many effects. Depending on the parameters, degradations of the luminosity can occur due to the hourglass effect. More serious is an enlargement of the collision energy spread, which may reduce the event rate and invalidate the monochromatization scheme.

DOI: 10.1103/PhysRevE.64.016502 PACS number(s): 29.20.Dh, 29.27.Bd, 41.75.Fr

I. INTRODUCTION

A τ-charm factory is being seriously considered [1]. To obtain a sufficient number of J/ψ particles, a monochromatization scheme has been actively studied [2]. Because the resonance width of the J/ψ particle is much smaller than the usual spread σ_w of the collision energy in e^+e^- storage rings, most collisions would not be useful for the experiment. Instead of reducing the energy spread of the beam, which is quite difficult, monochromatization has been proposed.

The idea of monochromatization is to reduce σ_w by producing a rather large dispersion D with opposite signs for the e^+ and e^- beams at the interaction point (IP). The dispersion at IP, however, is known to be a source of synchrotron-betatron coupling.

Often, the synchrotron degree of freedom is treated as a large heat bath, which is not affected at all [3–5]. Such a treatment might be reasonable when the dispersion is small, as in the case where it originates from machine errors. On the other hand, in the monochromatization scheme, the dispersion values might be well beyond the limit of this approximation. Hence, the effects on the synchrotron motion should also be considered, and the synchrotron and betatron degrees of freedom should be treated on equal footing.

In standard textbooks, such as Refs. [6,7], it appears that the definition of dispersion is based on the assumption that the energy of an electron is constant. This approach appears to be intuitively valid when the synchrotron tune value ν_z is close to zero, but we show that even this is not true. We also show that the usual definition of dispersion is not appropriate in the presence of a large dispersion at IP.

In simulation programs such as the beam-beam-code (BBC) described in [8], these effects are already included. A weak-strong simulation has been run on the basis of 3D (three-dimensional)-symplectic beam-beam mapping [9], which showed a satisfactory performance of the monochromatization scheme for the Beijing τ-Charm factory [10]. On the other hand, with only simulations it is difficult to understand the general properties of such a scheme.

In this paper we discuss all possible linear effects due to the presence of dispersion at the IP, while paying attention to the mutual interaction between the betatron and the synchrotron degrees of freedom within the weak-strong approximation of the linearized beam-beam force. Considering the role of the linear approximation in the usual beam-beam study, we can expect good insight concerning these effects by using this approximation. Such an analysis seems to be basic to understanding the fundamental structure of the problem but does not seem to have been performed with sufficient care [11]. Of course, this simplified calculation should not be applied directly to a realistic estimate of the effects.

This paper is organized as follows. In Sec. II, we discuss the symplectic effects. Section III is devoted to those effects associated with radiation (the beam sizes, etc.), including the luminosity and the energy resolution. Section IV is for discussion and conclusions. Some technical details are collected in the Appendix.

Preliminary results on the subject have been already published in a short form [12].

II. SYMPLECTIC EFFECTS

A. One-turn matrix

We start by constructing a one-turn matrix for single-particle motion, within the framework of the (weak-strong) linear symplectic dynamics for the case where dispersion exists at IP. We assume that there is only one IP and consider only the vertical and longitudinal motions.

The physical variables describing the betatron and synchrotron motions are

$$\mathbf{x}=(y,p,z,\varepsilon)\equiv(x_i), \tag{2.1}$$

where y is the vertical coordinate, $p=m\gamma_{rel}(dy/ds)/p_0$ is the vertical momentum normalized by the momentum p_0 of the reference particle (a constant), $z=s-ct(s)$, $\varepsilon=(E$

*Also at KEK, High Energy Research Organization, Tsukuba, Japan.

$-E_0)/E_0$, where E_0 is the energy of the reference particle, and γ_{rel} is the relativistic factor of the nominal particle energy.

The one-turn matrix from IP ($s=0_+$) to IP($s=0_-$), excluding the beam-beam kick, can be put in the following general form [13] as long as the motion is stable:

$$M(s)=H(s)B(s)\hat{M}_{arc}(s)B^{-1}(s)H^{-1}(s), \tag{2.2}$$

$$\hat{M}_{arc}(s)=\mathrm{diag}((\mu_y),r(\mu_z)), \quad B(s)=\mathrm{diag}(b_y,b_z), \tag{2.3}$$

$$b_{y,z}=\begin{pmatrix} \sqrt{\beta_{y,z}} & 0 \\ -\alpha_{y,z}/\sqrt{\beta_{y,z}} & 1/\sqrt{\beta_{y,z}} \end{pmatrix},$$

$$r(\mu)=\begin{pmatrix} \cos\mu & \sin\mu \\ -\sin\mu & \cos\mu \end{pmatrix}, \tag{2.4}$$

$$H=\begin{pmatrix} bI & h \\ \tilde{h} & bI \end{pmatrix}, \quad h=\begin{pmatrix} \zeta & \eta \\ \zeta' & \eta' \end{pmatrix},$$

$$\tilde{h}=jh^tj=\begin{pmatrix} -\eta' & \eta \\ \zeta' & -\zeta \end{pmatrix}. \tag{2.5}$$

Here $b=\sqrt{1-\det(h)}$, j is the 2×2 symplectic metric, $\mu=2\pi\nu$, and ν is the tune. Note that H, B, and $\hat{M}_{arc}$ are symplectic in the 4D sense.

The 4×4 symplectic matrix M has ten degrees of freedom. The number of Twiss parameters is also ten: the y and z modes have three parameters (ν,α,β) each, and the four parameters (η, η', ζ, and ζ') characterize the coupling between the two degrees of freedom. The η's are generalizations of the conventional dispersion D's, while the ζ's are to be called time dispersions.

The conventional dispersions D and D' as defined in Refs. [6,7] for example, assume that the energy of a particle is constant. They are defined as the closed orbit of an off-momentum particle. The conventional way is self consistent only when D and D' vanish in the cavities [14]. Then, η (η') is identical with D (D'), and ζ and ζ' vanish all over the ring. With the beam-beam interaction in the presence of D at IP, however, D and D' can be created in cavities even though they were zero before. This is why we need ζ's. Thus, in this case, it is not appropriate, to use D's but the (generalized) dispersion η is a natural extension of D, which (with ζ's) can work for general cases.

Now for simplicity, we assume that, without beam-beam interaction, the synchrotron-betatron coupling is absent and IP is a symmetric point with respect to the betatron and synchrotron motions,

$$M_{arc}=M(0_-,0_+)=H_0B_0\hat{M}^0_{arc}\ B_0^{-1}H_0^{-1}, \tag{2.6}$$

where $\hat{M}^0_{arc}$ is $\hat{M}_{arc}$ with $\mu_{y,z}=\mu^0_{y,z}$, B^0 is B with $\alpha_{y,z}=0$, and H_0 is H with $\eta=D_0$ and $\eta'=\zeta=\zeta'=0$. We have also implicitly assumed that the dispersion does not exist in cavities. The nominal synchrotron tune ν_z^0 is negative for conventional electron machines with a positive momentum compaction factor. We, however, consider both signs for ν_z^0 because of the option of the negative momentum compaction factor [15]. Note that the subfix or superfix 0 refers to all the unperturbed quantities evaluated without the beam-beam interaction.

We now introduce the beam-beam interaction at IP. For a head-on collision, the linearized beam-beam force is represented by the matrix

$$M_{bb}=\begin{pmatrix} 1 & 0 & 0 & 0 \\ -4\pi\xi_0/\beta_y^0 & 1 & 0 & 0 \\ 0 & 0 & 1 & 0 \\ 0 & 0 & 0 & 1 \end{pmatrix}, \tag{2.7}$$

$$\xi_0=\frac{Nr_e\beta_y^0}{2\pi\gamma_{rel}\sigma_y^0(\sigma_y^0+\sigma_x^0)}. \tag{2.8}$$

Here, ξ_0 is the vertical (nominal) beam-beam parameter, N is the number of particles in the strong beam, r_e is the classical electron radius, and σ_x^0 (σ_y^0) is the nominal horizontal (vertical) beam size.

For more realistic cases we should take into account the bunch-length effect [16], one possible way is to linearize the synchrotron-beam mapping [9]. For the sake of simplicity, however, we use Eq. (2.7) in the following. It seems convenient to introduce the effective betatron function β_y^{eff} as

$$\beta_y^{\mathrm{eff}}=\frac{\sigma_y}{\sigma_p}, \tag{2.9}$$

where $\sigma_p=\sqrt{\langle p^2\rangle}$, which agrees with β_y^0 when $D_0=0$ and $\xi_0\simeq0$. The typical parameters of the usual monochromatization scheme always satisfy the relation $\beta_y^{\mathrm{eff}}\gg\sigma_z$, σ_z being the bunch length. Therefore the bunch length effect is not important and this simplification is acceptable.

The full one-turn matrix (including the beam-beam interaction) can thus be written as

$$M=M_{bb}^{1/2}M_{arc}M_{bb}^{1/2}. \tag{2.10}$$

B. Linear instabilities

The (perturbed) tunes are obtained from the eigenvalues of M. These latter, in view of the symplecticity of M, can be readily computed as [12]

$$2\cos\mu_\pm=\cos\mu_y^0+\cos\mu_z^0-2\pi\xi_0(\sin\mu_y^0+\chi\sin\mu_z^0)\pm\sqrt{d}, \tag{2.11}$$

where

$$d=\{\cos\mu_y^0-\cos\mu_z^0-2\pi\xi_0(\sin\mu_y^0-\chi\sin\mu_z^0)\}^2 + 16\pi^2\xi_0^2\chi\sin\mu_y^0\sin\mu_z^0 \tag{2.12}$$

is the synchrotron tune-shift factor,

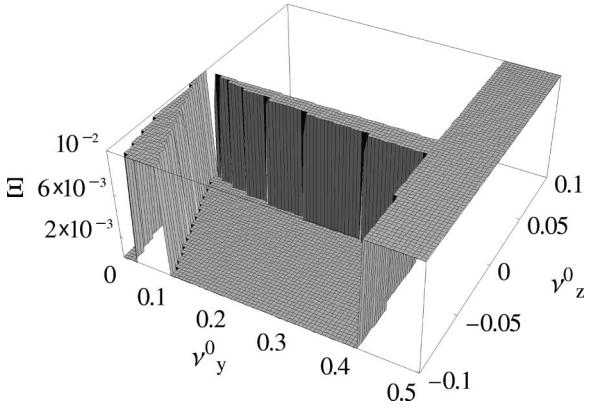

FIG. 1. The quantity Ξ (growth rate -1) as a function of ν_y^0 and ν_z^0 with $D_0=0.4$ m, $\xi_0=0.05$.

$$\chi=\frac{D_0^2}{\beta_y^0\beta_z^0}\simeq\frac{D_0^2\sigma_\varepsilon^0}{\beta_y^0\sigma_z^0}, \tag{2.13}$$

and σ_ε is the energy spread. The motion is stable if and only if $\cos\mu_\pm$ is real and $|\cos\mu_\pm|<1$. To the lowest order in ξ_0, we obtain

$$\nu_y^0\rightarrow\nu_y^0+\xi_0, \tag{2.14}$$

$$\nu_z^0\rightarrow\nu_z^0+\xi_0\chi. \tag{2.15}$$

Equation (2.14) is the well-known betatron tune shift, while Eq. (2.15) implies that a synchrotron tune shift also occurs due to the presence of D_0 at the IP.

Equations (2.14) and (2.15) imply that both tunes increase. Considering the motion of the eigenvalues on the unit circle in the complex plane, and from the fact that the motion becomes unstable only when two of the eigenvalues meet on the circle, we can expect that the system becomes unstable when one of the following conditions applies: (1) $\nu_y^0\lesssim$ half integers (betatron instability); (2) $\nu_z^0\lesssim$ half integers (synchrotron instability); (3) $\nu_z^0+\nu_y^0\lesssim$integers (synchro-betatron instability).

Using Eq. (2.11), the eigenvalues can be computed exactly. In Fig. 1 we plot the instability regions where the growth rate (largest absolute eigenvalue) exceeds unity in the (ν_y^0,ν_z^0) plane. Here (and hereafter, unless otherwise stated), the set of model parameters listed in Table I is used.

The three unstable regions mentioned above are clearly visible. The synchrotron-betatron instability corresponds to the case with $d<0$. The unstable regions become thicker for larger values of ξ_0 and D_0. As can be seen from the figure, a machine might be intrinsically more stable when $\nu_z^0>0$, because one can get rid of the synchrotron and synchrotron-betatron instabilities. Also note that the synchrotron-betatron instability region (both upper and lower edges) moves through the (ν_y^0,ν_z^0) plane as ξ_0 is changed, while the upper edges of the betatron and synchrotron instabilities regions stay fixed. This ''floating instability'' seems to be typical of the sum resonance in the beam-beam interaction [17].

TABLE I. Standard parameters used as examples in this paper.

β_y^0	0.03 m	β_z^0	26.3 m
ϵ_y^0	4×10^{-9} m	ϵ_z^0	3.8×10^{-6} m
σ_ε^0	3.8×10^{-4}	σ_z^0	0.01 m
T_y	1000	T_z	500

It is seen that the naive coasting (constant energy) beam approximation is not appropriate for $\nu_z^0\sim0$. In fact, for $\nu_z^0\lesssim0$, the motion is unstable: $\nu_z^0=0$ is a singular point and the coasting beam approximation is misleading.

The condition $\chi\ll1$ is equivalent to $(D_0\sigma_\varepsilon^0)^2/\beta_y^0\ll\epsilon_z^0$; for monochromatization to be useful, the beam size should be dominated by the dispersion contribution, so that we have

$$\epsilon_y^0\ll\frac{(D_0\sigma_\varepsilon^0)^2}{\beta_y^0}\ll\epsilon_z^0; \tag{2.16}$$

ϵ_z,ϵ_y being the emittances. It may be useful to note that the synchrotron tune shift is large for (1) large D_0, (2) large σ_ε^0, (3) small σ_z^0, (4) small β_y^0, and (5) small $|\nu_z^0|$. Items (3), (4), and (5) are general directions of design to obtain a large luminosity by making the beam size small while avoiding synchrotron-betatron side bands [18].

C. Twiss parameters

Twiss parameters are widely used in order to parametrize the one-turn matrix and to describe the properties of the lattice. Several definitions of Twiss parameters in the presence of synchrotron oscillations have been proposed. We follow the definition proposed in Ref. [13] where Twiss parameters are regarded as parameters that factorize and diagonalize the one-turn matrix. By this definition, dispersion is also included in the Twiss parameters. We use Eq. (2.10) and discuss how the beam-beam interaction in the monochromatization affects the Twiss parameters [14].

For later convenience, we first express the beam envelope matrix (in physical variables) $\sigma_{ij}\equiv\langle x_ix_j\rangle$ in terms of Twiss parameters. The normal mode variable $\mathbf{X}$ is defined as

$$\mathbf{X}=(HB)^{-1}\mathbf{x}. \tag{2.17}$$

Let us assume that the beam envelope matrix for the normal modes, $\mathcal{S}_{ij}\equiv\langle X_iX_j\rangle$, is

$$\mathcal{S}=\mathrm{diag}(\epsilon_u,\epsilon_u,\epsilon_v,\epsilon_v). \tag{2.18}$$

To evaluate the ϵ's, we should include the radiation effects, which is done in Sec. III. Equation (2.18) is a good approximation for the equilibrium distribution of an electron beam, provided that the effect of radiation is small [19].

From $\sigma=(HB)\mathcal{S}(HB)^t$, we obtain, after some algebra,

$$\langle y^2\rangle=b^2\beta_y\epsilon_y+\{\eta^2+(\beta_z\zeta-\alpha_z\eta)^2\}\beta_z^{-1}\epsilon_z,$$

$$\langle p^2\rangle=b^2\gamma_y\epsilon_y+\{\eta'^2\gamma_z+\beta_z\zeta'^2-2\alpha_z\eta'\zeta'\}\epsilon_z,$$

$$\langle z^2\rangle=\{\eta^2+(\alpha_y\eta_+\beta_y\eta')^2\}\beta_y^{-1}\epsilon_y+\beta_zb^2\epsilon_z,$$

$$\langle\varepsilon^2\rangle=\{\zeta^2+(\alpha_y\zeta+\beta_y\zeta')^2\}\beta_y^{-1}\epsilon_y+b^2\gamma_z\epsilon_z,$$

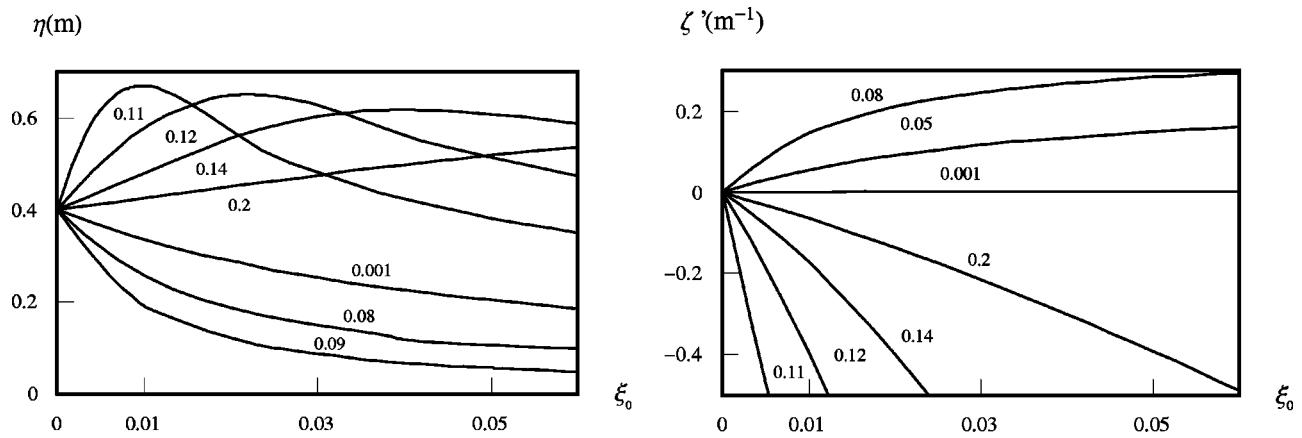

FIG. 2. η (left) and ζ' (right) as functions of ξ_0 for different values of ν_z^0 with $D_0=0.4$ m, $\nu_y^0=0.1$.

$$\langle yp\rangle = -\alpha_y b^2 \epsilon_y + \{\gamma_z \eta\eta' - \alpha_z(\eta\zeta' + \zeta\eta') + \beta_z \zeta\zeta'\}\epsilon_z,$$

$$\langle yz\rangle = -b(\alpha_y \eta + \beta_y \eta')\epsilon_y - b(\alpha_z \eta - \beta_z \zeta)\epsilon_z, \quad (2.19)$$

$$\langle y\varepsilon\rangle = b(\alpha_y \zeta + \beta_y \zeta')\epsilon_y + b(\gamma_z \eta - \alpha_z \zeta)\epsilon_z,$$

$$\langle p\varepsilon\rangle = -\{\zeta b + \alpha_y b(\alpha_y \zeta + \beta_y \zeta')\}\epsilon_y \beta_y^{-1} + \{\eta' b - \alpha_z b(-\alpha_z \eta' + \beta_z \zeta')\}\epsilon_z \beta_z^{-1},$$

$$\langle pz\rangle = \{b\eta + \alpha_y b(\alpha_y \eta + \beta_y \eta')\}\epsilon_y \beta_y^{-1} + b(\beta_z \zeta' - \alpha_z \eta')\epsilon_z,$$

$$\langle z\varepsilon\rangle = \{\eta\zeta + (\alpha_y \eta + \beta_y \eta')(\alpha_y \zeta + \beta_y \zeta')\}\beta_y^{-1}\epsilon_y - \alpha_z b^2 \epsilon_z,$$

where $\gamma=(1+\alpha^2)/\beta$.

The values of the Twiss parameters for M [Eq. (2.10)] at IP are now discussed.

In the middle of IP, due to symmetry, the dispersion D_0 makes η and ζ', and η' and ζ always zero. In Fig. 2, we show η and ζ' as functions of ξ_0 for various values of ν_z^0. When $\nu_z^0 \lesssim 0$, M can become unstable and we do not obtain η. Outside the instability region, η is almost an even function of ν_z^0. Here, we clearly see how η and ζ' depend on ν_z.

As can be seen in Fig. 2, ζ' grows up remarkably, particularly for $|\nu_z^0| \simeq \nu_y^0$. From Eq. (2.19), we might expect a dangerous growth of $\langle p^2\rangle$ and $\langle \varepsilon^2\rangle$ because of ζ' [see Eq. (2.19)]. Also, $\langle y\varepsilon\rangle$ (and $\langle pz\rangle$) can be greatly modified, which might affect the effective energy resolution of the monochromatic collision (see Sec. III C).

Concerning the (usual) Twiss parameters, α and β, because the IP is a symmetric point with respect to the betatron and synchrotron oscillations, α_y and α_z are zero, while β_y and β_z change with ν_z^0 as shown in Fig. 3.

III. LUMINOSITY AND COLLISION ENERGY SPREAD

In this section we discuss the combined effect of the synchrotron radiation, the linear optics, and the beam-beam kick on the beam sizes and related quantities.

With good accuracy, we might be able to obtain these latter quantities from Eq. (2.19) once we have computed the emittances ϵ_y and ϵ_z. This, however, is a rather indirect approach. We use a different formalism, where we first compute

$$\sigma_{ij} = \langle x_i x_j\rangle \quad (3.1)$$

and then derive the emittances from it [13]. Using this formalism, we do not need any detailed information concerning the lattice to calculate the effects of the beam-beam interaction, provided we have a formula for the one-turn map without the beam-beam interaction [19].

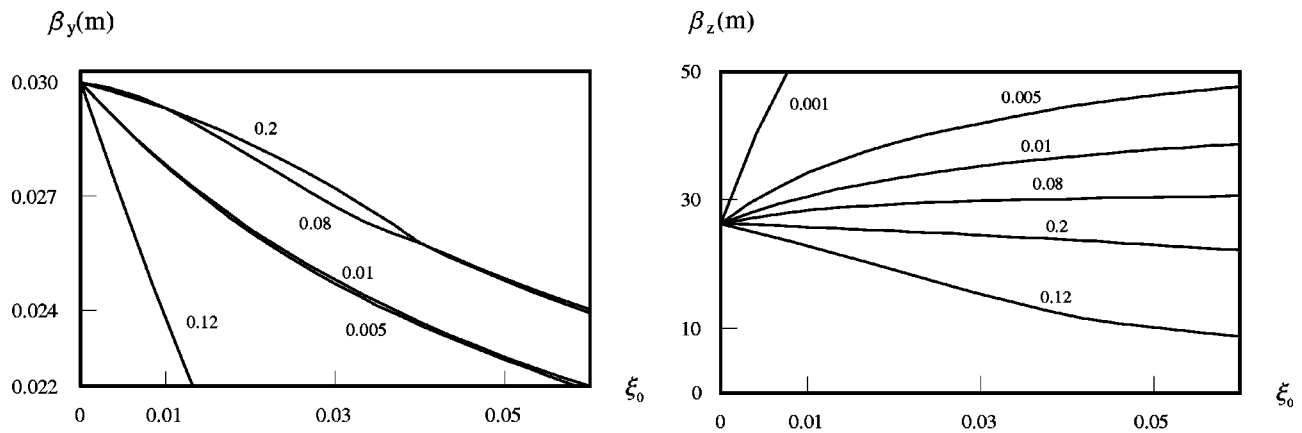

FIG. 3. β_y (left) and β_z (right) as functions of ξ_0 for different values of ν_z^0 with $D_0=0.4$ m, $\nu_y^0=0.1$.

A. Equilibrium envelope matrix

The effects of synchrotron radiation can be simply expressed in terms of the normal-mode variables, defined by Eq. (2.17), with respect to the unperturbed lattice, $\mathbf{X}_0 = (Y,P,Z,\Delta) \equiv (X_i^0)$, which is related to $\mathbf{x}$ as follows:

$$\mathbf{X}_0 = (H_0 B_0)^{-1} \mathbf{x}. \tag{3.2}$$

The mapping for $\mathbf{X}_0$ through the arc is then

$$\begin{pmatrix} Y \\ P \end{pmatrix}' = \lambda_y r(\mu_y^0) \begin{pmatrix} Y \\ P \end{pmatrix} + \sqrt{\epsilon_y^0 (1-\lambda_y^2)} \begin{pmatrix} g_1 \\ g_2 \end{pmatrix}, \tag{3.3}$$

$$\begin{pmatrix} Z \\ \Delta \end{pmatrix}' = \begin{pmatrix} 1 & 0 \\ 0 & \lambda_z^2 \end{pmatrix} r(\mu_z^0) \begin{pmatrix} Z \\ \Delta \end{pmatrix} + \sqrt{\epsilon_z^0 (1-\lambda_z^4)} \begin{pmatrix} 0 \\ g_3 \end{pmatrix}, \tag{3.4}$$

where g_i's are mutually independent random variables with $\langle g_i \rangle = 0$, $\langle g_i g_j \rangle = \delta_{ij}$, and $\lambda_{y,z} = \exp(-1/T_{y,z})$, T being the damping time (in units of the revolution time).

The change of the envelope matrix elements, $\mathcal{S}_{ij}^0 = \langle X_i^0 X_j^0 \rangle$, in the arc is then

$$\mathcal{S}^0 \to \mathcal{S}^0 = (\hat{\Lambda} \hat{M}_{arc}) \mathcal{S}^0 (\hat{\Lambda} \hat{M}_{arc})^t + (I - \hat{\Lambda}^2) \hat{E}_0, \tag{3.5}$$

where

$$\hat{E}_0 = \mathrm{diag}(\epsilon_y^0, \epsilon_y^0, \epsilon_z^0, \epsilon_z^0) \tag{3.6}$$

and

$$\hat{\Lambda} = \mathrm{diag}(\lambda_y, \lambda_y, 1, \lambda_z^2). \tag{3.7}$$

This treatment of radiation is not exact, but can be assumed to be a good approximation [19]. More precisely, one should use a tracking code to obtain the stochastic one-turn mapping [20].

From

$$\sigma = (H_0 B_0) \mathcal{S}^0 (H_0 B_0)^t, \tag{3.8}$$

we obtain a map for σ through the arc

$$\sigma \to (\Lambda M_{arc}) \sigma (\Lambda M_{arc})^t + (I - \Lambda^2) E_0, \tag{3.9}$$

where

$$\Lambda = (H_0 B_0) \hat{\Lambda} (H_0 B_0)^{-1}, \tag{3.10}$$

$$E_0 = (H_0 B_0) \hat{E}_0 (H_0 B_0)^t, \tag{3.11}$$

$$M_{arc} = (H_0 B_0) \hat{M}_{arc} (H_0 B_0)^{-1}. \tag{3.12}$$

By the beam-beam kick, σ is transformed as follows:

$$\sigma \to M_{bb} \sigma M_{bb}^t. \tag{3.13}$$

The equilibrium distribution (in the middle of the IP, in the laboratory frame) is thus a Gaussian distribution,

$$\psi(\mathbf{x}; s=0) = \frac{1}{\sqrt{(2\pi)^4 \det \sigma}} \exp\left(-\frac{1}{2} \sum_{i,j} \sigma_{ij}^{-1} x_i x_j \right), \tag{3.14}$$

where σ is the solution of the equation

$$\sigma = M_{bb}^{1/2} [(\Lambda M_{arc})(M_{bb}^{1/2}) \sigma (M_{bb}^{1/2})^t (\Lambda M_{arc})^t + (I - \Lambda^2) E_0] (M_{bb}^{1/2})^t. \tag{3.15}$$

The emittances are obtained from σ as follows:

$$\text{Eigenvalues}[J\sigma] = \{ i\epsilon_y, -i\epsilon_y, i\epsilon_z, -i\epsilon_z \}. \tag{3.16}$$

In Fig. 4 we plot the emittances $\epsilon_{y,z}$ as functions of ξ_0, for $\nu_z^0 = 0.08$ (left) and $\nu_z^0 = -0.08$ (right). It can be seen that the longitudinal emittance ϵ_z is considerably affected by the beam-beam force. This effect has usually been overlooked in the literature, where the synchrotron oscillation is assumed to be unaffected. Also, the vertical emittance ϵ_y increases quite rapidly.

In Fig. 5 we show some elements of the normalized envelope matrix, $\sigma_{ij}/\sigma_{ij}^0$, with $\sigma_{ij}^0 = \sigma_{ij}(\xi_0 = 0)$ as functions of ξ_0 for $\nu_z^0 = 0.08$ (left) and $\nu_z^0 = -0.08$ (right). For $D_0 = 0.4$ m, $\nu_y^0 = 0.05$ and $\nu_z^0 < 0$ (all other parameters being set as in Table I), instability sets in (growth rate > 1) for $\xi_0 \gtrsim 0.015\,774$ (instability threshold). It is thus not unexpected that all quantities blow up quickly when ξ_0 approaches this value.

Remarkably $\langle p^2 \rangle$ increases rapidly regardless of the sign of ν_z^0. This is consistent with the steep growth of ζ' shown in Fig. 2 and Eq. (2.19).

B. Luminosity

In this section we discuss the luminosity, based on the assumption that the distribution functions, $\psi^{\pm}(\mathbf{x})$, of the $e^{\pm}$ beams are Gaussian and are given by Eq. (3.14), σ being replaced by $\sigma^{\pm}$.

As is well known, for very short bunches colliding at s, the luminosity $\tilde{L}$ is given by

$$\tilde{L}(s) = \frac{N_+ N_- f_0}{2\pi \Sigma_x(s) \Sigma_y(s)}, \tag{3.17}$$

where x stands for the horizontal coordinates, $N^{\pm}$ is the number of particles in the $e^{\pm}$ bunch, f_0 is the collision frequency,

$$\Sigma_{x,y} = \sqrt{(\sigma_{x,y}^+)^2 + (\sigma_{x,y}^-)^2}, \tag{3.18}$$

$\sigma_x = \sqrt{\langle x^2 \rangle}$, $\sigma_y = \sqrt{\langle y^2 \rangle} = \sqrt{\sigma_{11}}$, and all quantities are measured at s. We further assume that the horizontal betatron function is very large at the IP and that $\sigma_x^{\pm}(s) = \sigma_x^{\pm}(0) \equiv \sigma_x^0$. Let us define the nominal luminosity as

$$L_0 = \tilde{L}(0). \tag{3.19}$$

For bunches colliding head-on with finite length $\sigma_z^{\pm}$, the luminosity reduction factor (the luminosity normalized to L_0) is given by

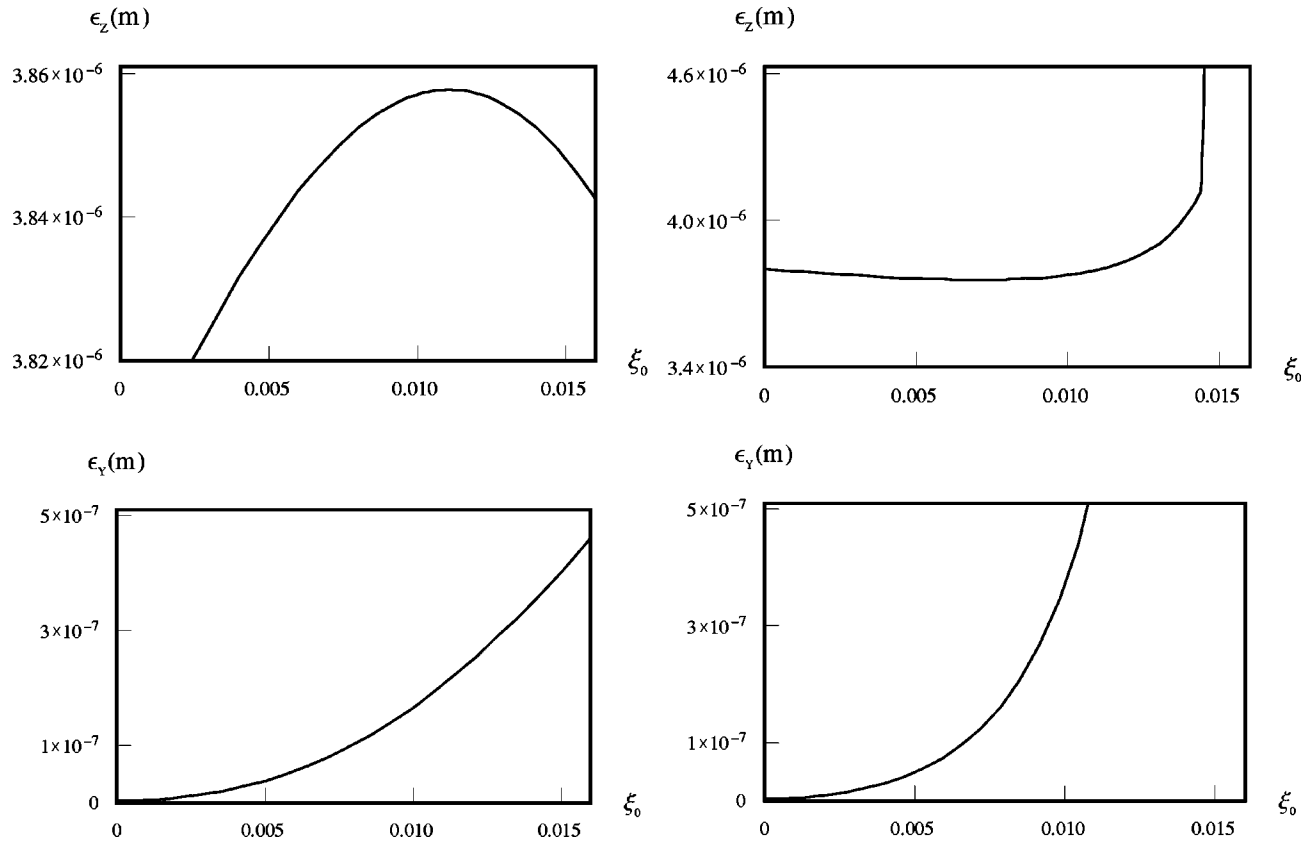

FIG. 4. Synchrotron emittances as functions of ξ_0 with $D_0=0.4$ m, $\nu_y^0=0.05$, $\nu_z^0=0.08$ (left), and $\nu_z^0=-0.08$ (right).

$$R_L=\frac{L}{L_0}=\frac{1}{L_0}\int_{-\infty}^{+\infty}\int_{-\infty}^{+\infty}dz_+\,dz_-\,\rho_+(z_+)\rho_-(z_-)\tilde{L}(s)$$
$$=\int_{-\infty}^{+\infty}ds\,C(s)\frac{\Sigma_y(0)}{\Sigma_y(s)}, \tag{3.20}$$

where $s=(z_+-z_-)/2$ and

$$C(s)=\sqrt{\frac{2}{\pi[(\sigma_z^+)^2+(\sigma_z^-)^2]}}\exp\left\{-\frac{2s^2}{(\sigma_z^+)^2+(\sigma_z^-)^2}\right\}. \tag{3.21}$$

The s dependence of Σ_y can be deduced from the following relations:

$$\sigma_{11}^{\pm}(s)=\sigma_{11}^{\pm}(0)^2+2\sigma_{12}^{\pm}(0)s+\sigma_{22}^{\pm}(0)s^2. \tag{3.22}$$

Assuming $\sigma_{12}^{+}(0)=-\sigma_{12}^{-}(0)$, we obtain

$$\Sigma_y(s)=\sqrt{\Sigma_y^2(0)+s^2\Sigma_p^2(0)}, \tag{3.23}$$

where

$$\Sigma_p=\sqrt{\sigma_{22}^{+}+\sigma_{22}^{-}}. \tag{3.24}$$

We assume hereafter that the two beams behave symmetrically so that, for example, $\Sigma_y=\sqrt{2}\sigma_y$. Hence,

$$R_L=\frac{1}{\sqrt{\pi}}\int_{-\infty}^{+\infty}\frac{du}{\sqrt{1+u^2/R_h^2}}\exp(-u^2), \tag{3.25}$$

where

$$R_h=\frac{\sigma_y(0)}{\sigma_z\sigma_p(0)}. \tag{3.26}$$

The integral is readily computed [21], yielding

$$R_L=\frac{R_h}{\sqrt{\pi}}K_0\left(\frac{R_h^2}{2}\right)\exp\left(\frac{R_h^2}{2}\right), \tag{3.27}$$

where K_0 is a modified Bessel function.

The hourglass effect [22,23] is more important for smaller R_h ($R_h\lesssim 1$), as can be seen from Fig. 6, where R_L is shown as a function of R_h. For this reason, R_h is called the hourglass ratio [12]. It can be written as

$$R_h=\frac{\beta_y^{\rm eff}}{\sigma_z}, \tag{3.28}$$

where $\beta_y^{\rm eff}$ is the effective betatron function, Eq. (2.9).

In Fig. 7, we show R_h as a function of ξ_0. A remarkable decrease of R_h is seen. For $\xi_0\simeq 0$, both η' and ζ vanish, as shown in Sec. II C, so that one obtains

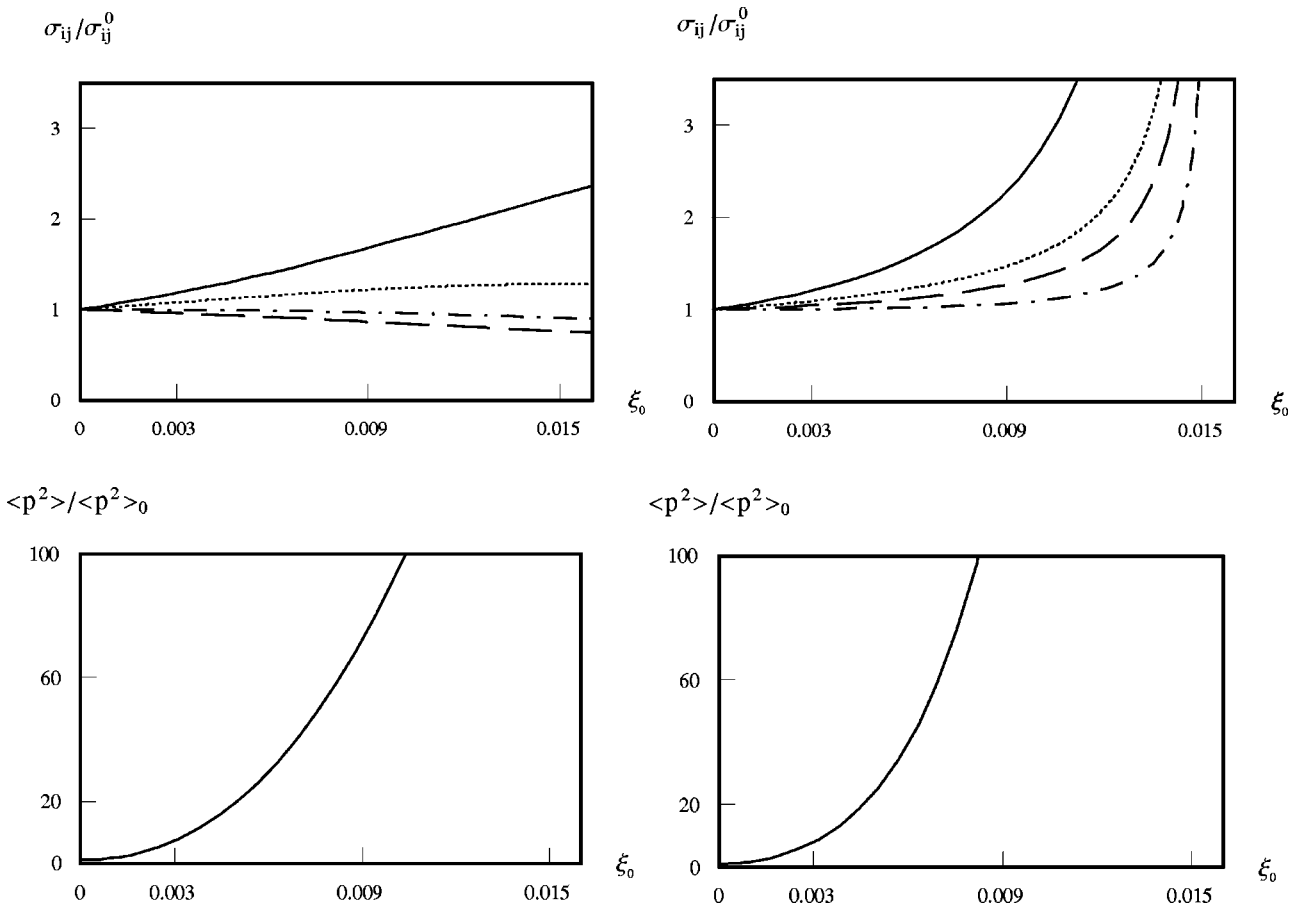

FIG. 5. Normalized elements of the envelope $\sigma_{ij}/\sigma_{ij}^0$ as functions of ξ_0 with $D_0=0.4$ m, $\nu_y^0=0.05$, $\nu_z^0=0.08$ (left), and $\nu_z^0=-0.08$ (right). Top: $\langle y^2\rangle/\langle y^2\rangle_0$ (solid line), $\langle z^2\rangle/\langle z^2\rangle_0$ (dashed line), $\langle \varepsilon^2\rangle/\langle \varepsilon^2\rangle_0$ (dashed-dotted line), $\langle y\varepsilon\rangle/\langle y\varepsilon\rangle_0$ (dotted line). Bottom: $\langle p^2\rangle/\langle p^2\rangle_0$.

$$R_h \simeq \frac{\beta_y^0}{\sigma_z^0}\sqrt{1+\frac{D_0^2}{\beta_y^0\epsilon_y^0}(\sigma_\varepsilon^0)^2} \quad (\xi_0 \simeq 0). \tag{3.29}$$

For $\xi_0 \simeq 0$, the beam size is dominated by dispersion in the monochromatization scheme. When ξ_0 increases, $\langle p^2\rangle$ increases rapidly as shown in Fig. 5, which makes $\beta_y^{\rm eff}$ and hence R_h small.

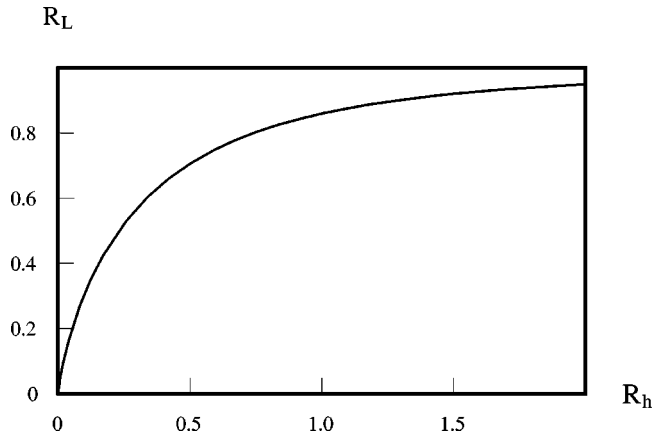

FIG. 6. Luminosity reduction factor R_L as a function of R_h.

This rapid decrease of R_h shows that, although the hourglass effect is not serious enough to reduce the luminosity considerably, one should pay careful attention to the bunch-length effect. At the same time, we note that R_h is still in the

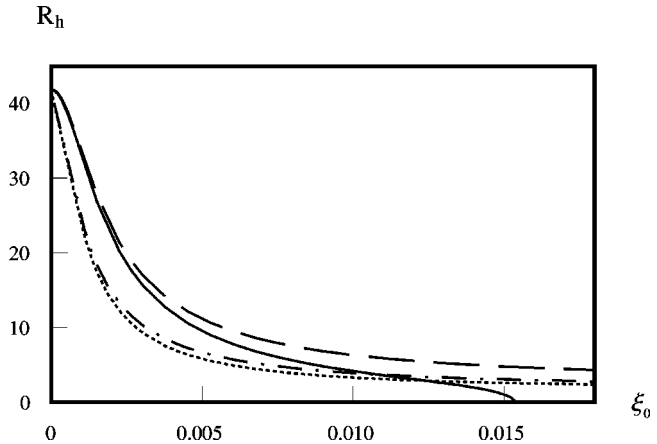

FIG. 7. Hourglass ratio R_h as a function of ξ_0 with $D_0=0.4$ m, $\nu_y^0=0.05$, and some values of ν_z^0: $\nu_z^0=0.03$ (dotted line), $\nu_z^0=-0.03$ (dash-dotted line), $\nu_z^0=0.08$ (dashed line), $\nu_z^0=-0.08$ (solid line). When $R_h \sim 1$, the hourglass effect is remarkable. The nominal value is $R_h^0=41$, and for $\nu_z^0=-0.08$, R_h becomes zero at the instability threshold $\xi_0 \approx 0.0158$.

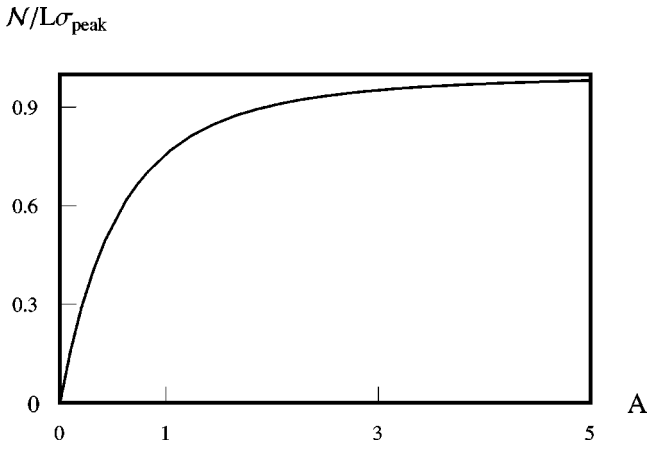

FIG. 8. Normalized event rate $\mathcal{N}/(L\sigma_{peak})$ as a function of A.

domain where the thin-lens approximation of the beam-beam kick, Eq. (2.7), is acceptable showing the self-consistence of our model.

C. Energy resolution

In monochromatization, the event rate $\mathcal{N}$ is the most important parameter. It depends on the luminosity L and the spread σ_w of the collision energy $E_+ + E_-$. Let $w = (\varepsilon_+ + \varepsilon_-) E_0$ be the deviation of the collision energy from the nominal value.

Usually $\mathcal{N}$ is related to the luminosity L by

$$\mathcal{N} = L\sigma, \tag{3.30}$$

where σ is the cross section of the event. For narrow resonances, however, σ depends very much on the collision energy w, so that $\sigma = \sigma(w)$. The event rate can, accordingly, be written as

$$\mathcal{N} = L \int_{\infty}^{+\infty} dw\, \Lambda(w)\sigma(w), \tag{3.31}$$

where $\Lambda(w)$ is the collision energy density function normalized to unity. When the cross section of the resonance is

$$\sigma(w) = \frac{\sigma_{peak}\Gamma^2}{w^2 + \Gamma^2}, \tag{3.32}$$

where σ_{peak} is the peak value of the cross section, Γ is the width of the resonance, and we assume that $\Lambda(w)$ is Gaussian with zero mean value and rms value σ_w, Eq. (3.31) is reduced to

$$\mathcal{N} = L\sigma_{peak}\sqrt{\pi} A\ \exp(A^2)\mathrm{erfc}(A), \tag{3.33}$$

where

$$A = \frac{\Gamma}{\sqrt{2}\sigma_w}. \tag{3.34}$$

A typical nominal value for τ-charm factories may be $A = 1/2$ [24]. In Fig. 8 the normalized event rate $\mathcal{N}/(L\sigma_{peak})$ is displayed as a function of A.

In a previous paper [12], we made a warning about a possible increase in the collision energy spread due to the beam-beam interaction. The discussion, however, was based on the assumption that the bunch-length effect can be ignored for the collision energy resolution. As shown above, R_h decreases remarkably, so that we may doubt whether the energy resolution increase might have been overestimated in the previous paper. To clarify this point, we extend our previous calculations to include the effect of a finite bunch length.

Let us start with the collision of very short bunches at position s. Let $\tilde{f}_{\pm}(y,\varepsilon)$ be the distribution function of the bunch after integration over p. The luminosity $\tilde{L}(s)$ can thus be put in the form [25]

$$\tilde{L}(s) = N_+ N_- f_0 \times \int_{-\infty}^{+\infty}\int_{-\infty}^{+\infty}\int_{-\infty}^{+\infty} dy\, d\varepsilon_+\, d\varepsilon_-\, \tilde{f}_+(y,\varepsilon_+)\tilde{f}_-(y,\varepsilon_-). \tag{3.35}$$

The distribution function of w can be written as

$$\tilde{\Lambda}(w) = \frac{N_+ N_- f_0}{\tilde{L}(s)}\int_{-\infty}^{+\infty}\int_{-\infty}^{+\infty}\int_{-\infty}^{+\infty} dy\, d\varepsilon_+\, d\varepsilon_- \times \delta(w - \varepsilon_+ - \varepsilon_-)\tilde{f}_+(y,\varepsilon_+)\tilde{f}_-(y,\varepsilon_-). \tag{3.36}$$

It is shown in the Appendix that assuming $\tilde{f}$ Gaussian, $\tilde{\Lambda}(w)$ is also Gaussian,

$$\tilde{\Lambda}(w) = \frac{1}{\sqrt{2\pi}\tilde{\sigma}_w(s)}\exp\left\{\frac{-[w - W(s)]^2}{2\tilde{\sigma}_w(s)^2}\right\}, \tag{3.37}$$

with the average

$$W = -\left(\frac{\sigma_{14}^+ - \sigma_{14}^-}{\sigma_{11}^+ + \sigma_{11}^-}\right)(\overline{y}_+ - \overline{y}_-) \tag{3.38}$$

and the second-order moment

$$\tilde{\sigma}_w^2(s) = \frac{(\sigma_{11}^+ + \sigma_{11}^-)(\sigma_{44}^+ + \sigma_{44}^-) - (\sigma_{14}^+ - \sigma_{14}^-)^2}{\sigma_{11}^+ + \sigma_{11}^-}. \tag{3.39}$$

For a thick bunch, the collision energy distribution is

$$\Lambda(w) = \frac{\int_{-\infty}^{+\infty} ds\, C(s)\tilde{L}(s)\tilde{\Lambda}(w)}{\int_{-\infty}^{+\infty} ds\, C(s)\tilde{L}(s)}, \tag{3.40}$$

the denominator being the luminosity. The collision energy spread σ_w is then given by

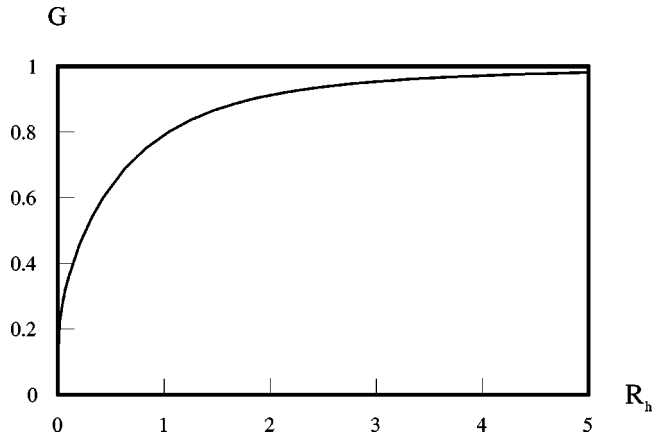

FIG. 9. G as a function of R_h.

$$\sigma_w^2=\frac{\int_{-\infty}^{+\infty} ds\, C(s)\tilde{L}(s)\tilde{\sigma}_w^2(s)}{\int_{-\infty}^{+\infty} ds\, C(s)\tilde{L}(s)}. \tag{3.41}$$

If we assume that the two beams are affected symmetrically, $\sigma_{11}^+=\sigma_{11}^-$, $\sigma_{44}^+=\sigma_{44}^-$ and $\sigma_{14}^+=-\sigma_{14}^-$, then

$$\tilde{\sigma}_w^2(s)=2\sigma_{44}[1-F(s)], \quad F(s)=\frac{\sigma_{14}^2}{\sigma_{11}\sigma_{44}}, \tag{3.42}$$

and the formula for σ_w becomes

$$\sigma_w^2=\frac{N^+N^-f_0\ \sigma_{44}(0)}{2\pi^{3/2}\sigma_x\sigma_y(0)L}\int_{-\infty}^{+\infty} du\frac{e^{-u^2}}{\sqrt{1+u^2/R_h^2}}\left[1-\frac{F(0)}{1+u^2/R_h^2}\right]. \tag{3.43}$$

The integral in Eq. (3.43) can be computed explicitly, yielding

$$\sigma_w^2=2\sigma_{44}(0)\{1-F(0)G(R_h)\}, \tag{3.44}$$

where

$$G(R_h)=R_h^2\left[\frac{K_1(R_h^2/2)}{K_0(R_h^2/2)}-1\right], \tag{3.45}$$

and K_1 is a modified Bessel function. In Fig. 9 we plot G versus R_h.

For $R_h\to\infty$ (short bunch), G becomes 1 and Eq. (3.44) gives $\sigma_w^2\to\tilde{\sigma}_w^2(0)$, while for $R_h\to 0$ (long bunch), G becomes 0 and $\sigma_w^2\to 2\sigma_{44}(0)$ as intuitively expected.

Let us turn to dynamics. As Fig. 7 shows, R_h decreases rapidly as a function of ξ_0 so that a substantial increase of σ_w may be foreseen. In Fig. 10 we plot the normalized collision energy spread $\sigma_w[2\sigma_{44}(0)]^{-1/2}$ versus ξ_0 for different values of ν_z^0. It is clear from the figure that the energy resolution increases rapidly with ξ_0, approaching its nominal value σ_ε^0; this happens regardless of the sign of ν_z^0. This behavior is similar to that obtained with the assumption of short bunches in Ref. [12]. As a consequence of the increase

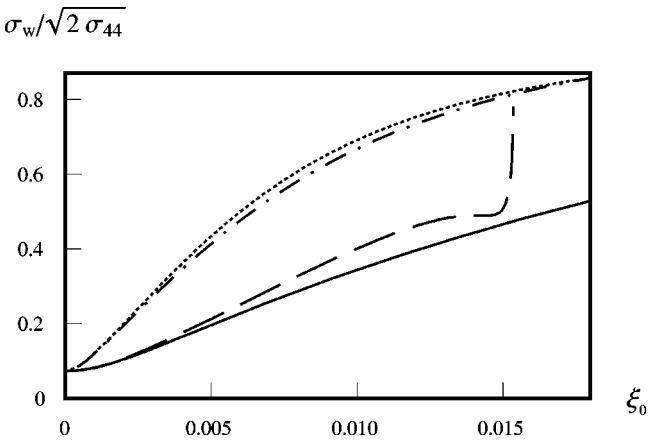

FIG. 10. Normalized collision energy spread as a function of ξ_0 with $D_0=0.4$ m, $\nu_y^0=0.05$, and some values of ν_z^0: $\nu_z^0=0.03$ (dotted line), $\nu_z^0=-0.03$ (dash-dotted line), $\nu_z^0=-0.08$ (dashed line), $\nu_z^0=0.08$ (solid line).

of σ_ε^0, the event rate $\mathcal{N}$ decreases from the nominal value as shown in Fig. 11. This decrease can be even more rapid or slightly slower for different ν_y as shown from Fig. 12.

Therefore, it turns out that the bunch length does not considerably affect the luminosity but the event rate.

The decrease of $\mathcal{N}$ is not only due to the reduction of R_h, but is also due to the decrease in the factor $F(0)$, as shown in Fig. 13, which enhances σ_w.

In conclusion, the rapid increase of the energy resolution σ_w with ξ_0 makes monochromatization less effective or even useless. This effect depends quite weakly on the betatron and synchrotron tunes as well as on all other parameters.

IV. DISCUSSION AND CONCLUSION

In the monochromatization scheme, through the large dispersion at the IP, the synchrotron and betatron motions influence each other, giving several nontrivial strong effects on the synchotron motion in addition to the well-known transverse effects for rather small values of ξ_0. These effects give several limits for the possible value of ξ_0. The first limit

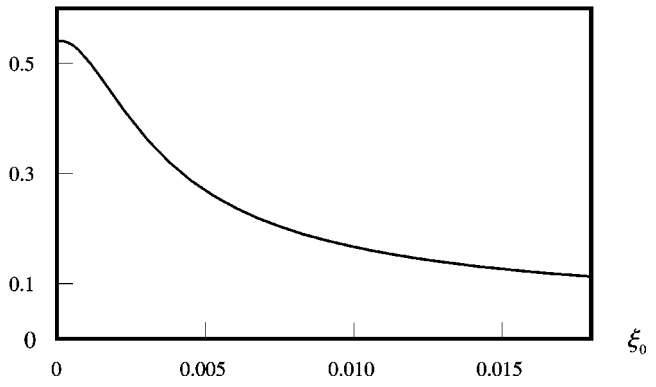

FIG. 11. Normalized event rate as a function of ξ_0 with $\nu_y^0=0.05$, $D_0=0.4$ m, and $\nu_z^0=0.08$.

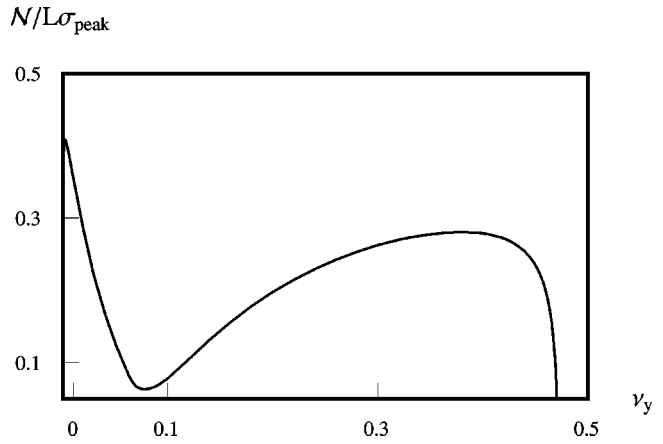

FIG. 12. Normalized event rate as a function of ν_y^0 with $\xi_0 = 0.015$, $D_0 = 0.4$ m, and $\nu_z^0 = 0.08$.

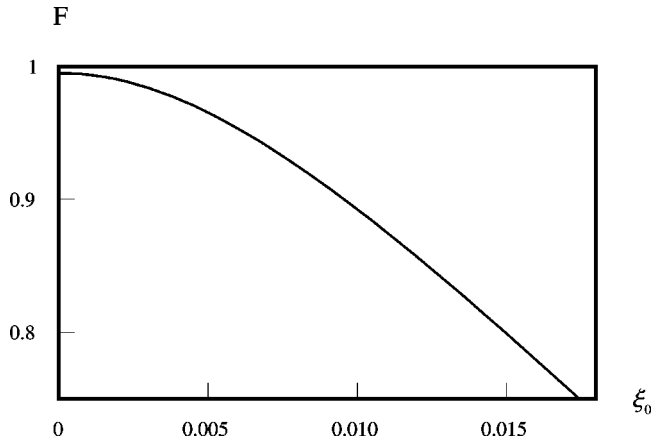

FIG. 13. $F(0)$ as a function of ξ_0 with $D_0 = 0.4$ m, $\nu_y^0 = 0.05$, $\nu_z^0 = 0.08$.

comes from the single-particle instability threshold, as discussed in Sec. II. The second comes from luminosity degradation. The most serious limit is due to an increase of the collision energy spread, which might invalidate the use of monochromatization.

Within the present analysis, it seems difficult to avoid such dangerous effects. The monochromatization scheme should be carefully optimized. A smaller value of D might be more useful; even if it gives a smaller value of $\mathcal{N}$ for small ξ_0, the degradation of $\mathcal{N}$ for a large value of ξ_0 might be less serious.

These conclusions might, however, come from an over simplification of the model. We need a more detailed analysis. First of all, the beam-beam force in the form of Eq. (2.7) is a linear approximation. In addition, the bunch-length effect is ignored; the force acts within the finite length and not as an impulse. It is theoretically possible to use the linear approximation of the beam-beam force including the bunch-length effects. It would, however, lose the simplicity of the model. A more detailed simulation, based on the symplectic beam-beam force [9], should be done while paying sufficient attention to the collision energy spread σ_w.

The present work, even if too much simplified to give a realistic design of a τ-charm factory, seems to be useful to understand potentially important issues before entering into a very detailed numerical analysis.

ACKNOWLEDGMENTS

The European Community is gratefully acknowledged for supporting S.P. during her stay at KEK. She also thanks the members of the KEK Accelerator Theory Group for their hospitality and help.

APPENDIX: ENERGY RESOLUTION FOR THE SLICES

Here, we derive Eqs. (3.38) and (3.39). We use the notation $(y,\varepsilon) = (x_1, x_2)$. From Eq. (3.36), we have

$$\tilde{\Lambda}(w) = \text{const} \times \int_{-\infty}^{+\infty}\int_{-\infty}^{+\infty}\int_{-\infty}^{+\infty} dx_1\, dx_2^+\, dx_2^- \times \delta(w - x_2^+ - x_2^-)\tilde{f}_+(x_1, x_2^+)\tilde{f}_-(x_1, x_2^-). \quad \text{(A1)}$$

Let $F_\pm(k_1,k_2)$ be the characteristic function of $\tilde{f}$

$$F(k_1,k_2) = \int_{-\infty}^{+\infty}\int_{-\infty}^{+\infty} dx_1\, dx_2\, e^{ik_i x_i}\tilde{f}(x_1,x_2) = \exp\left\{ ik_i\overline{x_i} - \frac{1}{2}A_{ij}k_ik_j \right\}, \quad \text{(A2)}$$

where repeated indices (i and j) are understood to be summed from 1 to 2 and

$$\overline{x_i} = \langle x_i \rangle, \quad A_{ij} = \langle (x_i - \overline{x_i})(x_j - \overline{x_j}) \rangle. \quad \text{(A3)}$$

We obtain

$$\tilde{\Lambda}(w) = \text{const} \times \int_{-\infty}^{+\infty}\int_{-\infty}^{+\infty} dk\, dp\, \tilde{f}_+(k,p)\tilde{f}_-(-k,p)e^{ipw}. \quad \text{(A4)}$$

The characteristic function of $\tilde{\Lambda}$ is

$$\lambda(p) = \int_0^{+\infty} dw\, e^{ipw}\tilde{\Lambda}(w) = \text{const} \times \exp\left\{ -i\frac{\Lambda_{12}}{\Lambda_{11}}Yp - \frac{1}{2}\left(\Lambda_{22} - \frac{\Lambda_{12}^2}{\Lambda_{11}} \right)p^2 \right\}, \quad \text{(A5)}$$

where $Y = \overline{x_1^+} - \overline{x_1^-}$, $\Lambda_{11} = A_{11}^+ + A_{11}^-$, $\Lambda_{12} = A_{12}^+ - A_{12}^-$, $\Lambda_{22} = A_{22}^+ + A_{22}^-$. This completes the derivation of Eqs. (3.38) and (3.39).

[1] IHEP-BTCF Report No 01, 1995 (unpublished); Yu. I. Alexahin, A. N. Dubrovin, and A. A. Zholents, in *Proceedings of the 2nd EPAC*, edited by P. Martin and P. Mandrillon (Editions Frontieres, Gif sur Yvette, 1990), p. 398; A.A. Zholents, in *Beam Dynamics Issues of High-Luminosity Asymmetric Collider Rings*, edited by Andrew M. Sessler, AIP Conf. Proc. No. 214 (AIP, New York, 1990), p. 592; A. Faus-Golfe and J. Le Duff, Nucl. Instrum. Methods Phys. Res. A **372**, 6 (1996). P. F. Beloshitsky, JINR Report No. EP-92-187, 1992 (unpublished); J. M. Jowett, in *Frontiers of Particle Beams: Factories with e^+e^- Rings*, edited by M. Denies, M. Month, B. Strasser, and S. Turner (Springer-Verlag, New York, 1994), and references therein.

[2] A. Renieri, Report No. INF-75/6(R), 1975 (unpublished).

[3] A. Piwinski, DESY Report No. 77/18, 1977 (unpublished); DESY Report No. H1/71-1, 1971 (unpublished).

[4] A.L. Gerasimov, D.N. Shatilov, and A.A. Zholents, Nucl. Instrum. Methods Phys. Res. A **305**, 25 (1991).

[5] Y. Kamiya and A.W. Chao, SLAC Report No. AP-10, 1983 (unpublished).

[6] E.D. Courant and H.S. Snyder, Ann. Phys. (N.Y.) **3**, 1 (1958).

[7] M. Sands, in *Physics with Interacting Storage Rings*, Proceedings of the International School of Physics ''Enrico Fermi,'' Course XLVI, Varenna, Italy, 1971, edited by B. Touschek (Academic Press, New York, 1971), p. 257.

[8] K. Hirata, CERN Report No. 97-57 (AP), 1997 (unpublished).

[9] K. Hirata, H. Moshammer, and F. Ruggiero, Part. Accel. **40**, 205 (1993).

[10] C. Zhang and K. Hirata, KEK Report No. 96-91, 1996 (unpublished).

[11] To the best of our knowledge, the only exception was Ref. [5]. Our approach in Sec. II is basically the same but more in detail.

[12] S. Petracca and K. Hirata, Phys. Rev. E **59**, R40 (1999).

[13] K. Ohmi, K. Hirata, and K. Oide, Phys. Rev. E **49**, 751 (1994).

[14] S. Petracca and K. Hirata, in *Proceedings of the 17th Particle Accelerator Conference*, edited by M. Comyn *et al*. (IEEE Press, New York, 1997), p. 1783.

[15] S.X. Fang *et al.*, Part. Accel. **51**, 15 (1995).

[16] S. Krishnagopal and R. Siemann, Phys. Rev. D **41**, 2312 (1990).

[17] K. Hirata and E. Keil, Part. Accel. **56**, 13 (1996).

[18] KEK Report No. 95-7, 1995 (unpublished).

[19] K. Hirata and F. Ruggiero, Part. Accel. **28**, 137 (1990); LEP Report No. 611, 1988 (unpublished).

[20] For example, in SAD [13], one can extract a one-turn map for the envelope σ_{ij} from realistic lattices. Even with respect to the normalized variables, the damping Λ and the diffusion $\hat{E}_0$ part usually have small off-diagonal elements.

[21] See, for example, M. Furmann, IEEE Proceedings of PAC, 91, edited by M. Allen (IEEE, Piscataway, NJ, 1991), p. 422.

[22] G. E. Fischer, SLAC Report No. SPEAR-154, 1972 (unpublished).

[23] SPEAR Storage Ring Group, IEEE Trans. Nucl. Sci. **NS-20**, 838 (1973).

[24] P.F. Beloshitsky, in *Beam Dynamics Issues for e^+-e^- Factories*, edited by L. Palumbo and G. Vignola, Frascati Physics Series Vol. 10 (INFN, Frascati, Italy, 1998), p. 457.

[25] M. Bassetti and J.M. Jowett, IEEE Proceedings of PAC, 87, edited by E. R. Lindstrom and L. S. Taylor (IEEE, Piscataway, NJ, 1987), p. 115.